

RESEARCH

Open Access



Introduction of human m⁶Am methyltransferase PCIF1 facilitates the biosynthesis of terpenoids in *Saccharomyces cerevisiae*

Guoli Wang^{1†}, Mingkai Li^{1†}, Bengui Fan^{1†}, Xiqin Liang¹, Jun Wang¹, Yanbing Shi¹, Qiusheng Zheng^{1*}, Defang Li^{1*} and Tianyue An^{1*}

Abstract

Background The application of synthetic biology techniques has been recognized as an efficient alternative for the biosynthesis of high-value natural products, and various metabolic engineering strategies have been employed to develop microbial cell factories. However, exploration of more efficient metabolic pathway optimization strategies is still required to further improve the producing potential of microbial cell factories to meet the industrial requirements.

Results In this study, we found that the introduction of human N⁶,2'-O-dimethyladenosine (m⁶Am) methyltransferase PCIF1 into *Saccharomyces cerevisiae* significantly promoted the biosynthesis of squalene, increased by 2.3-fold. Transcriptome analysis revealed that PCIF1 upregulated genes associated with glycolysis and acetyl-CoA biosynthesis pathways, and also activated the cell wall integrity mitogen-activated protein kinase (MAPK) pathway to improve the cell wall stress response. Importantly, PCIF1 expression notably enhanced squalene and sesquiterpenoid longifolene production in engineered yeast strains, with 2.3-fold and 1.4-fold higher increase, respectively.

Conclusion This study presents a PCIF1-based metabolic engineering strategy that could serve as an effective approach for the optimization of terpene biosynthesis in yeast cell factories.

Keywords *Saccharomyces cerevisiae*, m⁶Am methyltransferase, PCIF1, Terpene biosynthesis, Transcriptome, Metabolic engineering

[†]Guoli Wang, Mingkai Li and Bengui Fan contributed equally to this work.

*Correspondence:

Qiusheng Zheng

zqsyt@sohu.com

Defang Li

ldefang@163.com

Tianyue An

antianyue2007@126.com

¹Featured Laboratory for Biosynthesis and Target Discovery of Active Components of Traditional Chinese Medicine, School of Traditional Chinese Medicine, Binzhou Medical University, Yantai 264003, China



© The Author(s) 2025. **Open Access** This article is licensed under a Creative Commons Attribution-NonCommercial-NoDerivatives 4.0 International License, which permits any non-commercial use, sharing, distribution and reproduction in any medium or format, as long as you give appropriate credit to the original author(s) and the source, provide a link to the Creative Commons licence, and indicate if you modified the licensed material. You do not have permission under this licence to share adapted material derived from this article or parts of it. The images or other third party material in this article are included in the article's Creative Commons licence, unless indicated otherwise in a credit line to the material. If material is not included in the article's Creative Commons licence and your intended use is not permitted by statutory regulation or exceeds the permitted use, you will need to obtain permission directly from the copyright holder. To view a copy of this licence, visit <http://creativecommons.org/licenses/by-nc-nd/4.0/>.

Introduction

Natural products represent a critical source of bioactive compounds utilized in various industries, such as artemisinin and taxol in drug development [1–3], santalol and longifolene in cosmetics industries [4–6], and pyrethrin and azadirachtin in contemporary agriculture [7–9]. The application of synthetic biology techniques in the development of microbial cell factories has been recognized as an efficient alternative to traditional methodologies for producing these high-value natural products [10]. Successful production of many important chemicals is achieved by the employment of metabolic engineering strategies [11–14]. The widely implemented classical metabolic engineering strategies encompass promoter engineering, the optimization of key rate-limiting enzymes, the fusion of upstream and downstream genes within metabolic pathways, and “push-pull-block” strategy [15–19].

Currently, with the interdisciplinary collaboration between computer science and biotechnology, system level modelling, computational tools and machine learning approaches are frequently employed in metabolic engineering [20–23]. Although various metabolic engineering strategies have been developed for microbial biosynthesis of natural products, substantial improvement remains necessary to meet industrial production requirements. Consequently, further exploration of efficient metabolic pathway optimization strategies is still required to address future needs in the biosynthesis of natural products.

Post-transcriptional modifications of mRNA serve pivotal roles in regulating its splicing, transcription, translation, and stability [24–26]. N⁶-Methyladenosine (m⁶A), 5-methylcytosine (m⁵C) and pseudouridine (Ψ) modifications are found to be abundant in yeast mRNA [27–30], and among these modifications, the function of m⁶A is currently uncovered in detail. m⁶A modification can promote the decay and translation of mRNA, and regulates the meiosis process in diploid yeast and metabolism in haploid yeast [31–33]. Besides the above mRNA modifications, N⁶,2'-O-dimethyladenosine (m⁶Am) represents a specific type of RNA modification, occurring when the first nucleotide following the N⁷-methylguanosine cap is 2'-O-methyladenosine, which subsequently undergoes methylation at the N⁶ position to generate m⁶Am [34]. In mammalian cells, phosphorylated CTD interacting factor 1 (PCIF1) is responsible for catalyzing the m⁶Am modification [35]. The m⁶Am modification represents a key epigenetic change in mRNA, exerting a vital influence on the regulation of cellular metabolic pathways. This modification is known to stabilize mRNA and enhance its translation efficiency, which in turn modulates the expression of essential genes and affects various cellular processes [34, 36, 37]. By playing a pivotal role in the regulation of

gene expression, m⁶Am modification influences cellular metabolism by modulating specific metabolic pathways. For instance, it has been found to be enriched in multiple obesity- and metabolism-associated processes, with key metabolic genes undergoing m⁶Am methylation in obese mice [37, 38].

During the fermentation, microbial cells experience stresses related to gene expression and metabolic flux. These stresses would cause negative effects to the growth and behavior of the engineered strains. For example, changes in environmental condition can cause the intracellular genetic perturbation and lower the accuracy of gene expression. Stabilizing the gene expression serves as an effective strategy to maintain cellular homeostatic state. Therefore, an approach is needed to stabilize the gene expression of these microbial cells. As PCIF1-mediated m⁶Am modification was reported to stabilize the mRNA expression and improve the transcription and translation in human cells, although it is absent in yeast [39, 40], we wondered whether the heterologous expression of PCIF1 would help to improve the performance of these microbial cell factories. To verify this hypothesis, PCIF1 was overexpressed in *Saccharomyces cerevisiae* to assess its impact on yeast gene expression and metabolism. Results indicated that PCIF1 introduction led to a promotion in squalene production, increase by 2.3-fold. Transcriptome sequencing revealed that PCIF1 upregulated genes associated with glycolysis and acetyl-CoA biosynthesis pathways. Subsequently, squalene and the sesquiterpene compound longifolene were chosen as the target compounds, and engineered strains were developed. PCIF1 expression enhanced the production of squalene to 274.10 ± 12.92 mg/L, representing a 2.3-fold increase, and promoted the yield of sesquiterpenoid longifolene to 16.23 ± 0.30 mg/L, a 1.4-fold improvement. This study presents a PCIF1-based metabolic engineering strategy that could serve as an effective approach for optimizing terpene biosynthesis in yeast.

Methods

Plasmid and strain construction

The genomic DNA (gDNA) of *S. cerevisiae* was extracted utilizing the FastPure Plant DNA Isolation Mini Kit (Vazyme Biotech, China). The endogenous yeast genes *ERG12*, *ERG10*, *ERG13*, *ERG8*, *ERG19*, *ID11*, *ERG20*, and *ERG9* were amplified from the gDNA by using 2 × Phanta Max Master Mix (Vazyme Biotech, China) and inserted into the pEASY[®]-Blunt cloning vector (TransGen Biotech, China) for sequence verification. The *PCIF1*, *EfmvaE*, and *PsLS* genes were synthesized by General Biol (China). Genes involved in the mevalonate (MVA) pathway were separately constructed into pESC-TRP/HIS/URA vectors. The expression cassette for *PCIF1* was assembled by overlap PCR, linking the *PCIF1* gene with

Table 1 Plasmids and strains constructed in this work

Plasmids	Description	Source
pESC-TRP	Yeast expression vector	Agilent Technologies
pESC-LEU	Yeast expression vector	Agilent Technologies
pESC-HIS	Yeast expression vector	Agilent Technologies
pESC-URA	Yeast expression vector	Agilent Technologies
pCRCT	Yeast CRISPR/cas9 vector	Addgene
pEASY-Blunt	Gene cloning vector	TransGen Biotech
pTP01	Replace the GAL10p with PGK1p in pESC-LEU	This study
pTP02	Insert PCIF1 into pTP01	This study
pTP03	Insert <i>EfmvaE</i> into pESC-TRP	This study
pTP04	Insert <i>ERG12</i> into pTP03	This study
pTP05	Insert <i>ERG10</i> into pESC-HIS	This study
pTP06	Insert <i>EfmvaS</i> into pTP05	This study
pTP07	Insert <i>ERG8</i> into pESC-URA	This study
pTP08	Insert <i>ERG19</i> expression cassette into pTP07	This study
pTP09	Insert <i>ID11</i> into pTP08	This study
pTP10	Ligate <i>ERG20</i> to pEASY-Blunt	This study
pTP11	Insert <i>ERG20</i> ^{F96W/N127W} into pESC-URA	This study
pTP12	Insert <i>ERG9</i> into pTP11	This study
pTP13	Insert HXT1p to pESC-URA	This study
pTP14	Replace the HIS marker with KanMX in pESC-HIS	This study
pTP15	Insert PsLS into pTP14	This study
pTP16	Insert <i>ERG20</i> ^{F96W/N127W} into the upstream of PsLS in pTP16	This study
Strains	Genotype	Source
CEN.PK2-1 C	<i>MATa leu2-3,112 ura3-52 trp1-289 his3-Δ1 MAL2-8c SUC2</i>	ATCC
TP01	CEN.PK2-1 C <i>NDT80::LEU</i> <i>PGK1p-PCIF1-ADH1t</i>	This study
TP02	CEN.PK2-1 C <i>BTS1::TRP GAL10p-EfmvaE-ADH1t-GAL1p-ERG12-CYC1t</i>	This study
TP03	TP02 <i>DPP1::HIS GAL10p-ERG10-ADH1t-GAL1p-EfmvaS-CYC1t</i>	This study
TP04	TP03 308a:: <i>GAL10p-ERG8-ADH1t-GAL10p-ERG19-CYC1t-GAL1p-ID11-ADH1t</i>	This study
TP05	TP04 <i>LPP1::URA GAL10p-ERG20^{F96W/N127W}-ADH1t-GAL1p-ERG9-CYC1t</i>	This study
TP06	TP05 <i>NDT80::LEU</i> <i>PGK1p-PCIF1-ADH1t</i>	This study
TP07	TP04 <i>ERG9p::URA HXT1p</i>	This study
TP08	TP07:: pTP15	This study
TP09	TP07:: pTP16	This study
TP10	TP09 <i>NDT80::LEU</i> <i>PGK1p-PCIF1-ADH1t</i>	This study

PGK1p promoter, TDH1t terminator and the LEU selection marker. *ERG20* was mutated to *ERG20*^{F96W/N127W} using Fast Site-Directed Mutagenesis Kit (Tiangen, China) and subsequently integrated into the pESC-URA vector together with *ERG9*. The selection marker of pESC-HIS was substituted with KanMX, after which the *PsLS* gene was constructed into this modified vector.

The expression cassettes corresponding to each individual gene were amplified from their corresponding vectors and subsequently introduced into yeast cells by utilizing Frozen-EZ Yeast Transformation II Kit (Zymo, USA). Notably, *ERG8*, *ERG19*, and *ID11* were incorporated into the 308a locus of the yeast genome through the CRISPR/Cas9 technology, while the remaining genes were integrated at their designated locations within the yeast genome via homologous recombination. The plasmids and strains developed in this part are listed in Table 1, and the primers are listed in Table S1.

Growth curve determination by microbial growth curve analyzer

Six single colonies of the positive yeast strain were inoculated into YPD yeast medium containing 20 g/L glucose as the carbon source, and the culture concentration was adjusted to an OD₆₀₀ of 0.1. A volume of 500 μL of the yeast suspension was transferred to a 48-well plate and incubated at 30 °C with shaking at 700 rpm. And samples were periodically taken at designated time intervals using microbial growth curve analyzer (Scientz, China) to measure the OD₆₀₀ values. And a growth curve was generated based on the accumulated data.

Semiquantitative RT-PCR

Total RNA was isolated from cultured yeast cells using Trizol reagent (Invitrogen, USA) and subsequently reverse-transcribed into cDNA utilizing the HiScript II Q RT SuperMix for qPCR kit (Vazyme Biotech, China). UBC6 was employed as the reference gene, and semi-quantitative RT-PCR was conducted using Phanta Max Super-Fidelity DNA Polymerase (Vazyme Biotech, China). The primer sequences used in this analysis are listed in Table S1.

Shake flask fermentation

A single colony of positive yeast strain was first introduced into 5 mL of SD medium, where they were incubated at 30 °C with shaking at 220 rpm for a period ranging between 12 and 16 h. Subsequently, a suitable volume of the culture was transferred into 50 mL of SD medium, adjusting the OD₆₀₀ to 0.1.

For triterpene compound fermentation, the previously mentioned medium was cultured under the same conditions of 30 °C and 220 rpm for 120 h, after which the culture underwent harvesting. In the case of longifolene

fermentation, the culture was initially incubated at 30 °C and 220 rpm for 24 h, following which 15% (v/v) sterile nonane was added. Fermentation then proceeded under the same conditions for a further 120 h.

Compound detection

Triterpene compounds detection: The culture was centrifuged at 3,000 rpm for 5 min. Yeast cells were harvested and subsequently boiled in a lysis buffer consisting of 20% (v/v) potassium hydroxide and 50% (v/v) ethanol for 10 min. The resulting lysate was then combined with the supernatant, and an equivalent volume of *n*-hexane was introduced, followed by a settling period lasting 48 h. The upper organic layer was then subjected to drying using a rotary evaporator. The dried sample was treated with 50 µL of *N*-Methyl-*N*-(trimethylsilyl) trifluoroacetamide at 80 °C for 30 min prior to gas chromatography-mass spectrometry (GC-MS) analysis. The GC-MS analysis utilized a 19,091 S-433UI gas chromatography column paired with a 5977B single quadrupole mass spectrometer equipped with an electron ionization source at 70 eV. Helium served as the carrier gas, with the flow rate maintained at 1.0 mL/min. The injection volume for the sample was 1 µL, operated in splitless or split mode at a 50:1 ratio. The initial temperature was programmed to 160 °C, held for 1 min, then raised to 280 °C at a rate of 30 °C/min and maintained for 10 min, with a subsequent final increase to 300 °C at a rate of 2 °C/min, where it was held for 5 min.

Longifolene detection: Following fermentation, 1 mL of the upper organic phase was extracted, filtered, and subsequently analyzed using GC-MS. The conditions for detection were as follows. Helium, serving as the carrier gas, maintained a flow rate of 1.0 mL/min. The sample injection volume was set to 1 µL, with the analysis conducted in splitless mode. The initial temperature was programmed at 50 °C and sustained for 3 min, after which it was elevated to 70 °C at a rate of 20 °C/min, where it was held for 1 min. Finally, the temperature was increased to 300 °C at a rate of 15 °C/min and held for 10 min.

RNA sequencing

Cells of CEN.PK2-1 C and TP01 strains, during their exponential phase, were collected through centrifugation at 3,000 rpm/min and 4 °C. Total RNA extraction was carried out using Trizol reagent (Invitrogen, USA), followed by quantification with a NanoDrop 2000 spectrophotometer. The integrity of the extracted RNA was evaluated using the Agilent RNA Nano 6000 kit. mRNA was isolated from the total RNA using Thermo Fisher Scientific DynabeadsTM Oligo(dT)25 mRNA purification beads. Transcriptome sequencing was subsequently performed on the Illumina Novaseq platform by Novogene Corporation (Beijing, China).

Statistical analysis

Data processing and statistical evaluations were conducted using GraphPad Prism 8 software. All experiments were carried out in triplicate, with the results presented as mean ± standard deviation ($M \pm SD$). Statistical significance was defined as $p < 0.05$.

Results

PCIF1 introduction promotes the biosynthesis of squalene in *S. cerevisiae*

To explore the role of m⁶Am methyltransferase PCIF1 in *S. cerevisiae* metabolism, the *PCIF1* gene expression module was integrated into the genome of *S. cerevisiae* strain CEN.PK2-1 C, generating strain TP01. The expression of the *PCIF1* gene in this engineered yeast strain was first assessed, with semiquantitative RT-PCR results confirming its high expression in yeast cells (Fig. 1A). Growth curves were then monitored by using microbial growth curve analyzer and a fed-batch fermentation to evaluate the influence of PCIF1 on yeast growth. The data revealed that, compared to the WT strain, strain TP01 exhibited a growth advantage than the WT strain (Fig. 1B and Fig. S1). This suggests that the introduction of PCIF1 influenced the growth of yeast, which was consistent with the reports that PCIF1 impacted the growth of human cells [41, 42].

Further analysis involved the cultivation of both CEN.PK2-1C and TP01 strains in shake flasks to assess their metabolite profiles. GC-MS analysis demonstrated a significant enhancement of squalene biosynthesis in the TP01 strain (Fig. 1C and Fig. S2). By employing standard curves for squalene (Fig. S3), it was calculated that the TP01 strain produced 2.50 ± 0.07 mg/L of squalene, corresponding to 2.3-fold increases, compared to the WT strain (Fig. 1D). These findings indicate that the integration of the PCIF1 gene promotes the biosynthesis of triterpene compounds in yeast.

PCIF1 markedly affects the expression of genes involved in yeast metabolism and stress response

To further elucidate the mechanism by which PCIF1 enhances triterpene biosynthesis in yeast, a transcriptome sequencing analysis was conducted on the TP01 and WT strain. The analysis revealed 1,821 differentially expressed genes (DEGs), with 909 genes upregulated and 921 genes downregulated in comparison to the WT strain (Fig. S4A). Notably, 79 genes were uniquely expressed in the WT, whereas 60 genes were uniquely expressed in the TP01 strain (Fig. S4B). Gene Ontology (GO) enrichment analysis demonstrated that these DEGs were predominantly involved in oxidation-reduction processes, carbohydrate metabolism, phosphorus metabolic processes, transferase activity, and oxidoreductase activity (Fig. 2A). Importantly, the introduction of PCIF1 had

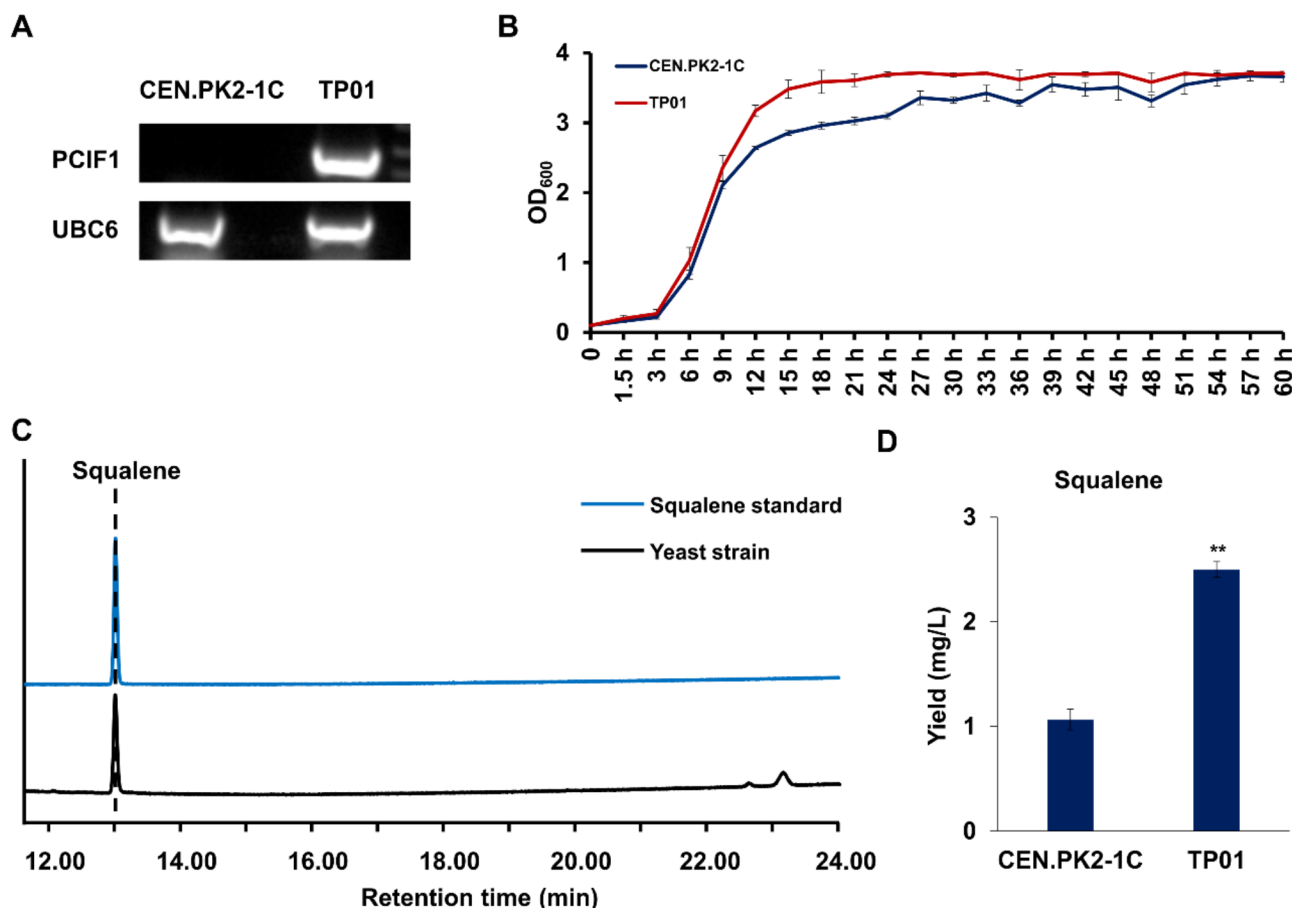


Fig. 1 PCIF1 promoted the biosynthesis of squalene in yeast. **(A)** Expression detection of *PCIF1* by semiquantitative RT-PCR. **(B)** The growth curves of CEN.PK2-1 C and TP01 strain. **(C)** GC-MS detection of triterpene in yeast strain. **(D)** The production of squalene in different strains. The asterisks indicate significant differences (** $p < 0.01$, * $p < 0.05$)

a profound effect on the oxidation-reduction processes within yeast cells. Kyoto Encyclopedia of Genes and Genomes (KEGG) enrichment analysis indicated that the DEGs were primarily enriched in pathways associated with the biosynthesis of secondary metabolites, carbon metabolism, amino acid biosynthesis, and glycolysis/gluconeogenesis (Fig. 2B). Of these, the biosynthesis of secondary metabolites pathway exhibited the highest degree of enrichment. Collectively, these findings underscore the pivotal role of PCIF1 in regulating oxidation-reduction processes, carbon metabolism, secondary metabolism, and amino acid synthesis in *S. cerevisiae*.

During fermentation and cultivation, yeast cells are exposed to numerous stress factors, including nutrient depletion and the accumulation of toxic by-products, which result in the build-up of reactive oxygen species (ROS) and disturbances in energy metabolism, consequently restricting the biosynthesis of desired compounds. Previous reports have shown that the inhibition of ROS accumulation and the preservation of cell wall integrity are essential strategies employed by yeast cells to manage stress conditions [43–45]. Here, through

transcriptome analysis, it was discovered that the over-expression of PCIF1 led to an enrichment of functional genes involved in cellular redox processes (Fig. 2A). Moreover, differential gene expression analysis revealed an upregulation in the expression of many genes encoding signaling molecules in the cell wall integrity (CWI) mitogen-activated protein kinase (MAPK) pathway, including Pkc1, Mkk1 and Slt2 (Fig. 3B). These findings imply that PCIF1 might improve the stress tolerance of yeast cells by influencing the genes involved in the stress response.

PCIF1 promoted squalene production through increasing the biosynthesis of acetyl-CoA

To determine the factors contributing to the elevated production of triterpene compounds in the TP01 strain, the squalene synthesis pathways were examined. A comparative analysis of the triterpene biosynthesis pathway and the upstream MVA pathway was carried out between the TP01 and WT strains. Unexpectedly, transcriptome data did not reveal significant increase in gene expression levels within these two pathways, and even some enzymes

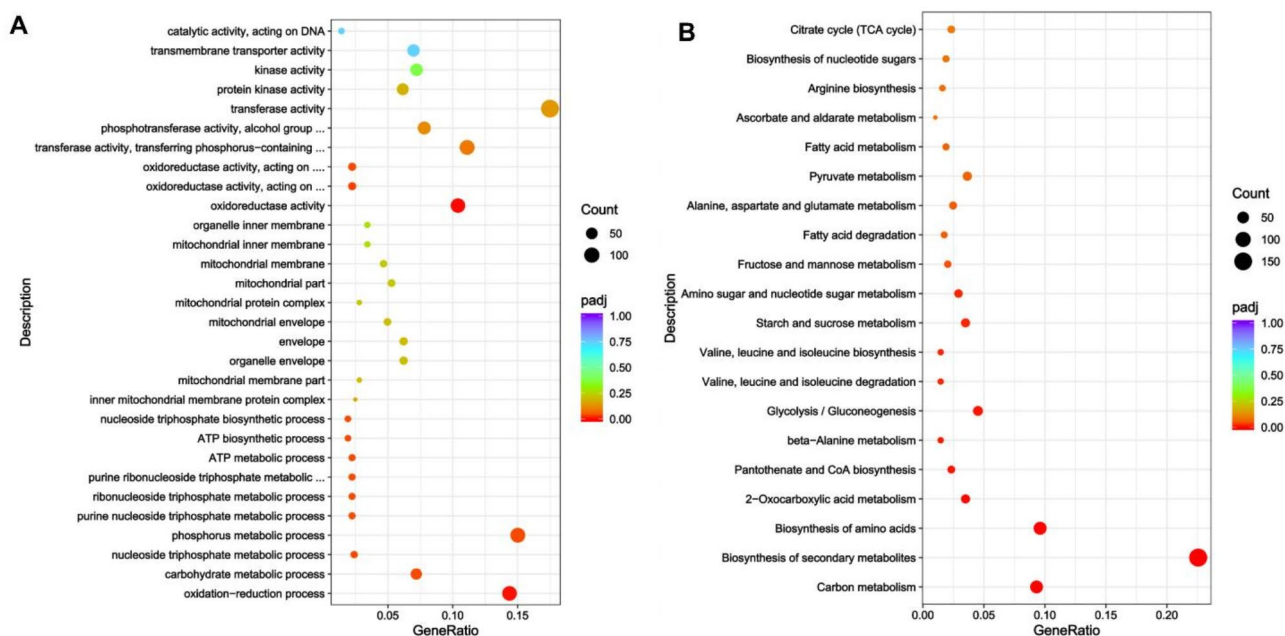


Fig. 2 Transcriptome analysis of PCIF1 transformed strain and CEN.PK2-1 C. **(A)** GO analysis of DEGs in different yeast strains. **(B)** KEGG analysis of DEGs in different yeast strains

showed down-regulated expression levels (Table S2). As acetyl-CoA serves as the precursor of MVA, attention was subsequently directed toward the acetyl-CoA synthesis pathway. In yeast, pyruvate, a glycolytic product, can be converted into acetyl-CoA through either the pyruvate dehydrogenase (PDH) complex in mitochondria or PDH bypass in cytosol [46–48]. Also, acetyl-CoA can be derived via β -oxidation of fatty acids in peroxisomes [48]. Transcriptome sequencing demonstrated that genes in β -oxidation, including *POX1* and *POT1*, were down-regulated (Table S2), while most genes involved in the glycolytic pathway in the TP01 strain exhibited upregulated expression, including *HXK1*, *TDH1*, *TDH3*, *PGK1*, *GPM1*, and *CDC19* (Fig. 4). In the two pathways leading from pyruvate to acetyl-CoA, genes coding for the pyruvate decarboxylase complex, such as *PDA1*, *PDB1*, and *LAT1*, were upregulated (Fig. 4). Similarly, aldehyde dehydrogenases involved in the PDH bypass, including *Ald3*, *Ald4*, and *Ald5*, were also found to be upregulated (Fig. 4). Meanwhile, *CTP1*, the transporter encoding gene responsible for the transportation of acetyl-CoA in the form of citrate from mitochondria to cytosol was also upregulated (Table S2). These findings indicate that PCIF1 promotes triterpene compound biosynthesis by upregulating both the glycolysis and acetyl-CoA synthesis pathways.

PCIF1 increased squalene production in engineered yeast

To assess whether PCIF1 can sustain its capacity to elevate triterpene production in engineered strains and potentially serve as a viable metabolic engineering

strategy for triterpene biosynthesis, engineered strains with enhanced triterpene output were developed, and triterpene yields were compared pre- and post-introduction of PCIF1. In *S. cerevisiae*, the MVA pathway initiates with acetyl-CoA. Acetyl-CoA is first converted by acetoacetyl-CoA thiolase *Erg10* and 3-hydroxy-3-methylglutaryl-CoA (HMG-CoA) synthase *Erg13* into HMG-CoA. This HMG-CoA is subsequently reduced by HMG-CoA reductase to generate MVA, which undergoes further conversion to isopentenyl pyrophosphate (IPP) through a series of phosphorylation and decarboxylation reactions catalyzed by *Erg12*, *Erg8*, and *Erg19*. IPP is then isomerized to dimethylallyl pyrophosphate (DMAPP) by IPP isomerase *Idi1* [49–51]. Among them, previous studies have shown that *EfmvaS*^{A110G}, a mutant of *EfmvaS* encoding HMG-CoA synthase from *Enterococcus faecalis*, alongside the HMG-CoA reductase *EfmvaE*, displays increased conversion efficiency [52–54]. Therefore, to optimize the MVA pathway, genes encoding the aforementioned enzymes were overexpressed, culminating in the engineered strain TP04 (Fig. 5A).

Within the subsequent steps of the triterpene biosynthesis pathway, IPP and DMAPP are first converted into farnesyl pyrophosphate (FPP) by the *Erg20*, after which FPP is further transformed into squalene by the squalene synthase *Erg9* [55]. Previous research indicates that the *Erg20*^{F96W/N127W} double mutant possesses greater catalytic efficiency and specificity [56]. To improve the triterpene biosynthesis pathway, both *Erg20*^{F96W/N127W} and *Erg9* were overexpressed (Fig. 5A), leading to the creation of the engineered strain TP05. Shake flask fermentation

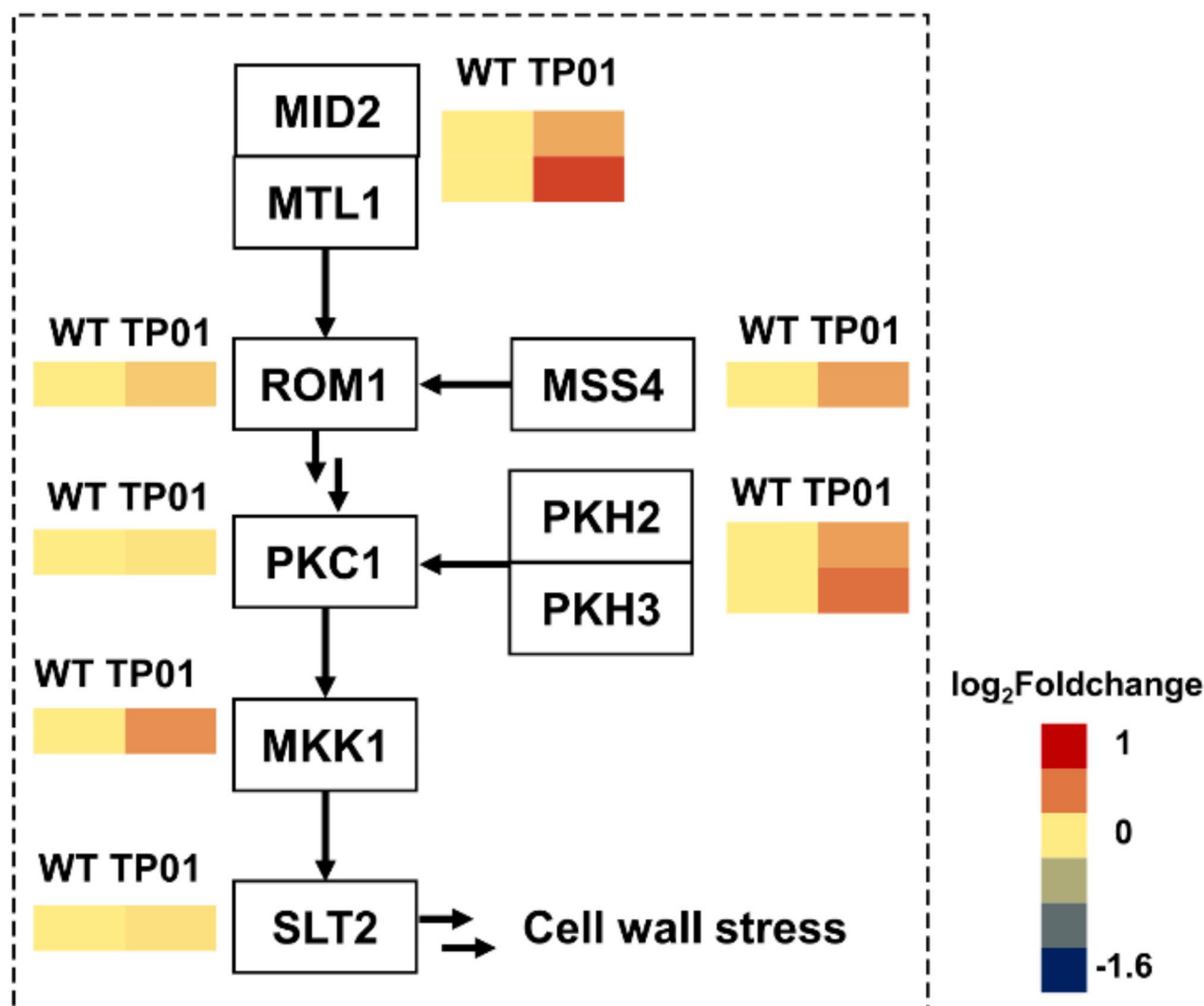


Fig. 3 The expression of genes involved in cell wall stress response in different yeast strains

of this strain, alongside analysis using the squalene standard curve (Fig. S5), revealed that 120.59 ± 5.24 mg/L of squalene was produced (Fig. 5B). Following this, the PCIF1 expression module was inserted into the genome, resulting in strain TP06. Fermentation assays conducted with TP06 demonstrated a squalene production level of 274.10 ± 12.92 mg/L (Fig. 5B), representing a 2.3-fold increase compared to strain TP05. These findings illustrate that PCIF1 is capable of substantially enhancing squalene production in engineered yeast.

PCIF1 enhances sesquiterpene biosynthesis in engineered yeast

Given the ability of PCIF1 to stimulate the biosynthesis of triterpene compounds in yeast, it is important to explore whether it can similarly enhance the biosynthesis of other terpenes. Longifolene, a tricyclic sesquiterpene obtained from *Pinus palustris*, is an aromatic compound

with notable antibacterial and antioxidant activities and is widely utilized in the pharmaceutical, fuel, fragrance, and cosmetic industries [8, 57, 58]. As such, longifolene was chosen as a represented sesquiterpene to assess the effect of PCIF1 on its biosynthesis. In strain TP04, where the MVA pathway was optimized, the native promoter of *ERG9* was substituted with the glucose-repressible HXT1p promoter, producing strain TP07 (Fig. 6A). Subsequently, the longifolene synthase gene *PsLS* from *P. sylvestris* [7] was transformed into strain TP07, resulting in strain TP08. Using the longifolene standard curve (Fig. S6), it was determined that strain TP08 produced 2.35 ± 0.39 mg/L of longifolene during shake flask fermentation (Fig. 6B and Fig. S7).

To further improve the efficiency of longifolene production, a fusion protein consisting of *Erg20*^{F96W/N127W} and *PsLS*, linked by a peptide linker GSG, was constructed and introduced into TP07, resulting in strain TP09.

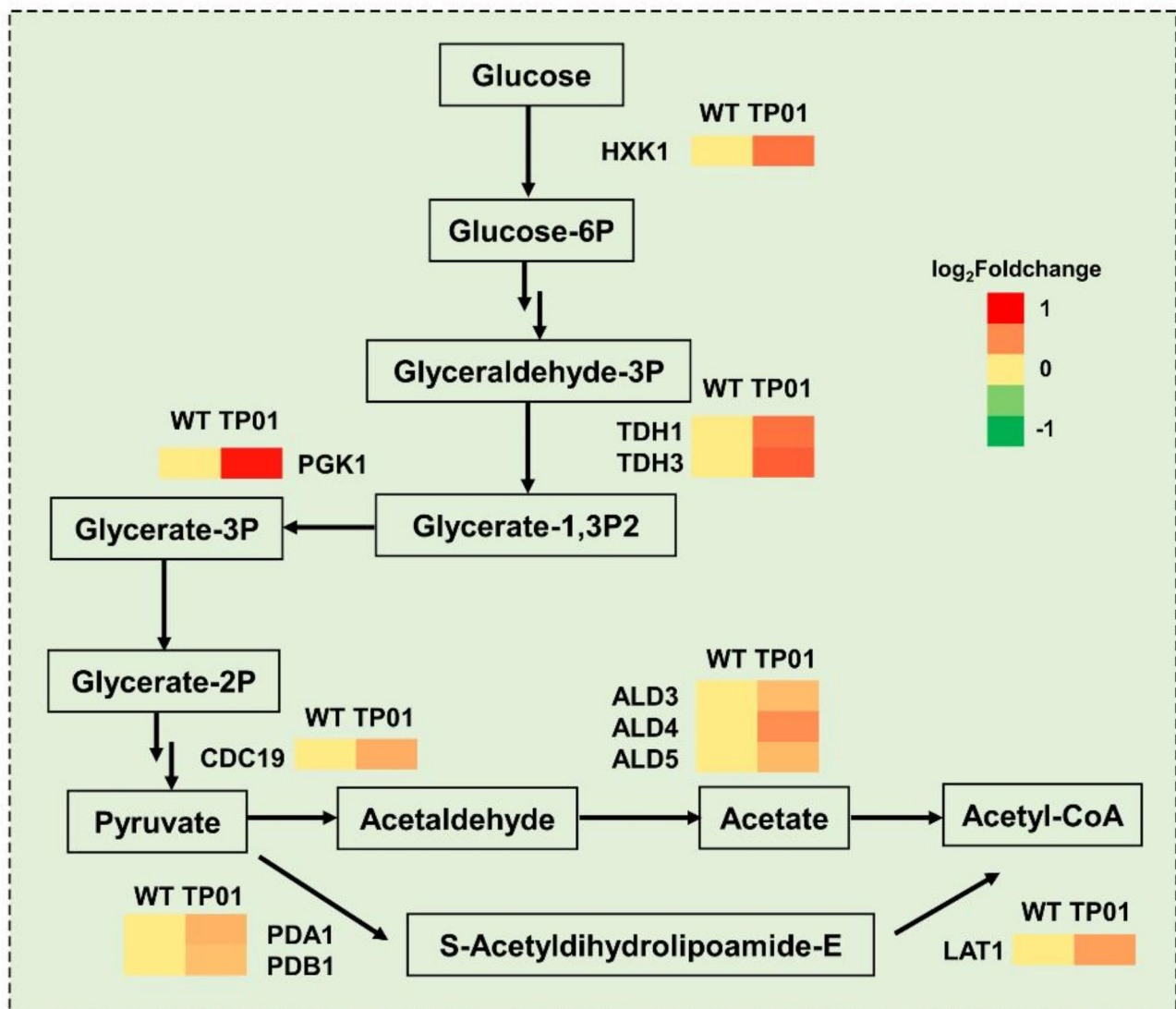


Fig. 4 The expression of genes involved in glycolysis. HXK1, hexokinase 1; TDH1/3, glyceraldehyde-3-phosphate dehydrogenase; PGK1, phosphoglycerate kinase; CDC19, pyruvate kinase; ALD3/4/5, aldehyde dehydrogenases; PDA1, pyruvate dehydrogenase; PDB1, pyruvate dehydrogenase; LAT1, dihydrolipoamide acetyltransferase

Fermentation analysis of TP09 showed that longifolene production reached 11.46 ± 1.01 mg/L (Fig. 6C). Following this, the *PCIF1* expression cassette was inserted into the genome of strain TP09, generating strain TP10. Fermentation results revealed that this strain produced 16.23 ± 0.30 mg/L of longifolene (Fig. 6C), representing a 1.4-fold increase over strain TP10. These results suggest that the *PCIF1*-based metabolic engineering approach enhances sesquiterpene production in engineered yeast strains.

Discussion

Previously, m⁶Am modification has been implicated in cellular adaptation to hypoxia and glucose metabolism [34, 37]. Transcriptome studies have demonstrated that

this modification markedly alters the metabolic pathways of cancer cells, such as those in gastric and colorectal cancers, by regulating genes critical to cancer cell metabolism, thereby promoting cellular growth and proliferation [59, 60]. These findings underscore the importance of m⁶Am modification not only in transcriptional regulation but also in its broader impact on cellular functions through modulation of specific metabolic pathways. In this study, it was observed that when the human m⁶Am methyltransferase *PCIF1* was expressed in *S. cerevisiae*, it markedly influenced cellular redox processes and was involved in yeast carbon metabolism, secondary metabolism, and amino acid synthesis (Fig. 2). Additionally, *PCIF1* was found to activate the MAPK pathway, which is

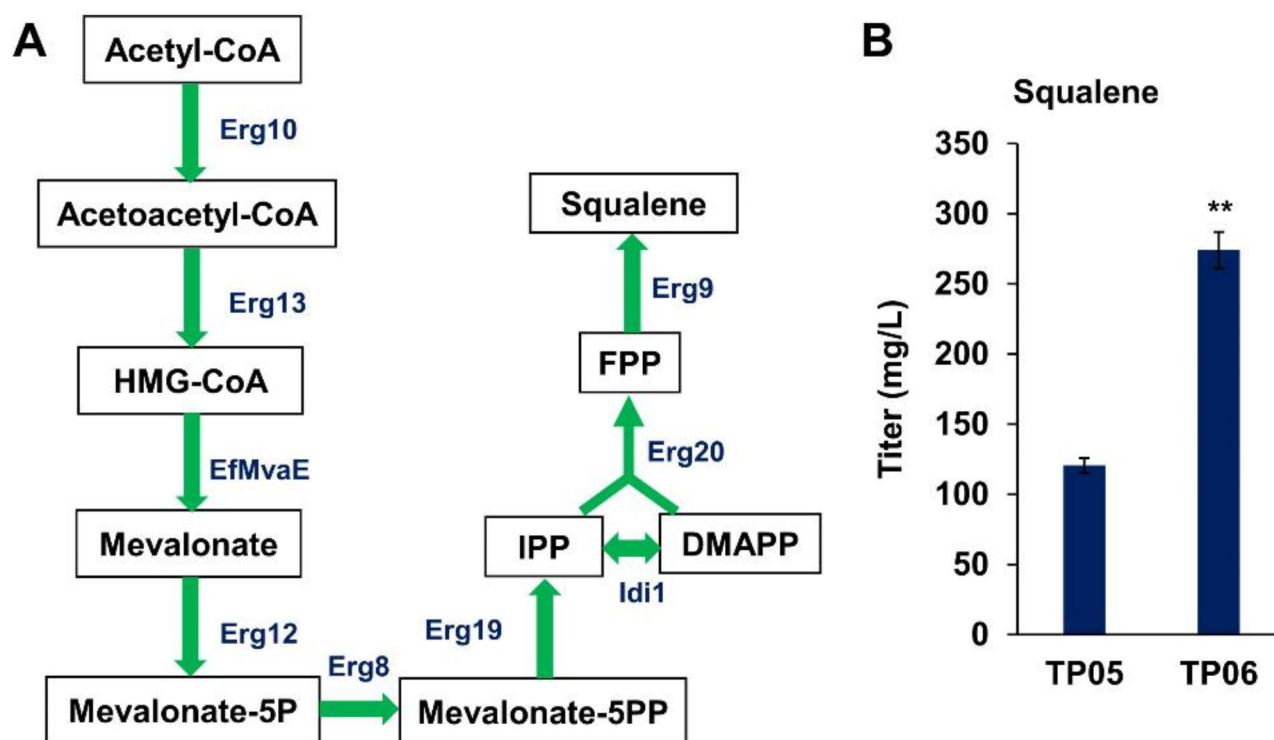


Fig. 5 PCIF1 significantly promoted squalene production in engineered yeast. **(A)** The optimization of squalene biosynthesis pathway. Erg10, acetoacetyl-CoA thiolase; Erg13, HMG-CoA synthase; EfMvaE, HMG-CoA reductase from *E. faecalis*; Erg12, mevalonate kinase; Erg8, phosphomevalonate kinase; Erg19, mevalonate pyrophosphate decarboxylase; Idl1, isopentenyl diphosphate: dimethylallyl diphosphate isomerase; Erg20, farnesyl pyrophosphate synthetase; Erg9, squalene synthase. **(B)** The squalene production in different yeast strains. The asterisks indicate significant differences (** $p < 0.01$, * $p < 0.05$)

capable of enhancing cell wall integrity, thereby increasing yeast resistance during fermentation (Fig. 3).

Significantly, this research reveals for the first time that PCIF1 is involved in the regulation of glycolysis and acetyl-CoA synthesis pathways, leading to the upregulation of key enzymes in these pathways and the enrichment of the acetyl-CoA pool. It is widely acknowledged that acetyl-CoA acts as a precursor in the biosynthesis of numerous compounds, including isoprenoids, terpenes, fatty acids and their derivatives, and polyketides [61]. Several prior studies have documented enhanced production of these target compounds by augmenting acetyl-CoA synthesis [62]. For instance, the enhanced supply of acetyl-CoA and NADPH by inhibiting the acetyl-CoA competing pathway promoted the betulinic acid titer from 88.07 ± 5.83 mg/L to 166.43 ± 1.83 mg/L, increased by 1.89-fold in engineered yeast strain [63]. An improved acetyl-CoA supply by the combination of phosphoketolase (PK) and phosphotransacetylase (PTA) pathways led to the production of 50.29 mg/L β -carotene, improved by 80% [64]. The introduction of an alternative cytoplasmic acetyl-CoA pathway to *Yarrowia lipolytica* resulted in a 32% enhanced β -ionone titer [65]. The present study confirms that the PCIF1-induced enrichment of acetyl-CoA can stimulate terpene biosynthesis, 2.3-fold and 1.4-fold increase in squalene and longifolene production,

respectively, in engineered yeast strains (Fig. S8). Thus, the regulation of acetyl-CoA biosynthesis through PCIF1 presents a promising metabolic engineering strategy for acetyl-CoA-derived compounds, particularly terpenes, to enhance the efficiency of target compound synthesis. Future research will focus on further investigating the role of PCIF1 in promoting the production of other acetyl-CoA-derived compounds in microbial cell factories to broaden its applications in natural product biosynthesis.

Transcriptome sequencing of the PCIF1-transformed strain revealed that the expression levels of enzymes involved in the two pathways responsible for converting the glycolytic product pyruvate into acetyl-CoA, including the PDH complex and the PDH bypass, were markedly upregulated. Consequently, these two pathways present potential targets for further enhancement in future engineering efforts aimed at increasing acetyl-CoA production. For example, building on a previously reported strategy for optimizing the PDH bypass, overexpression of Ald6 and the mutant acetyl-CoA synthetase SeACS^{L641P} from *Salmonella enterica* could be employed to further promote acetyl-CoA synthesis [66], which would further improve the biosynthesis of its derived compounds.

In one of our previous reports, we overexpressed another similar methyltransferase, the m⁶A modification

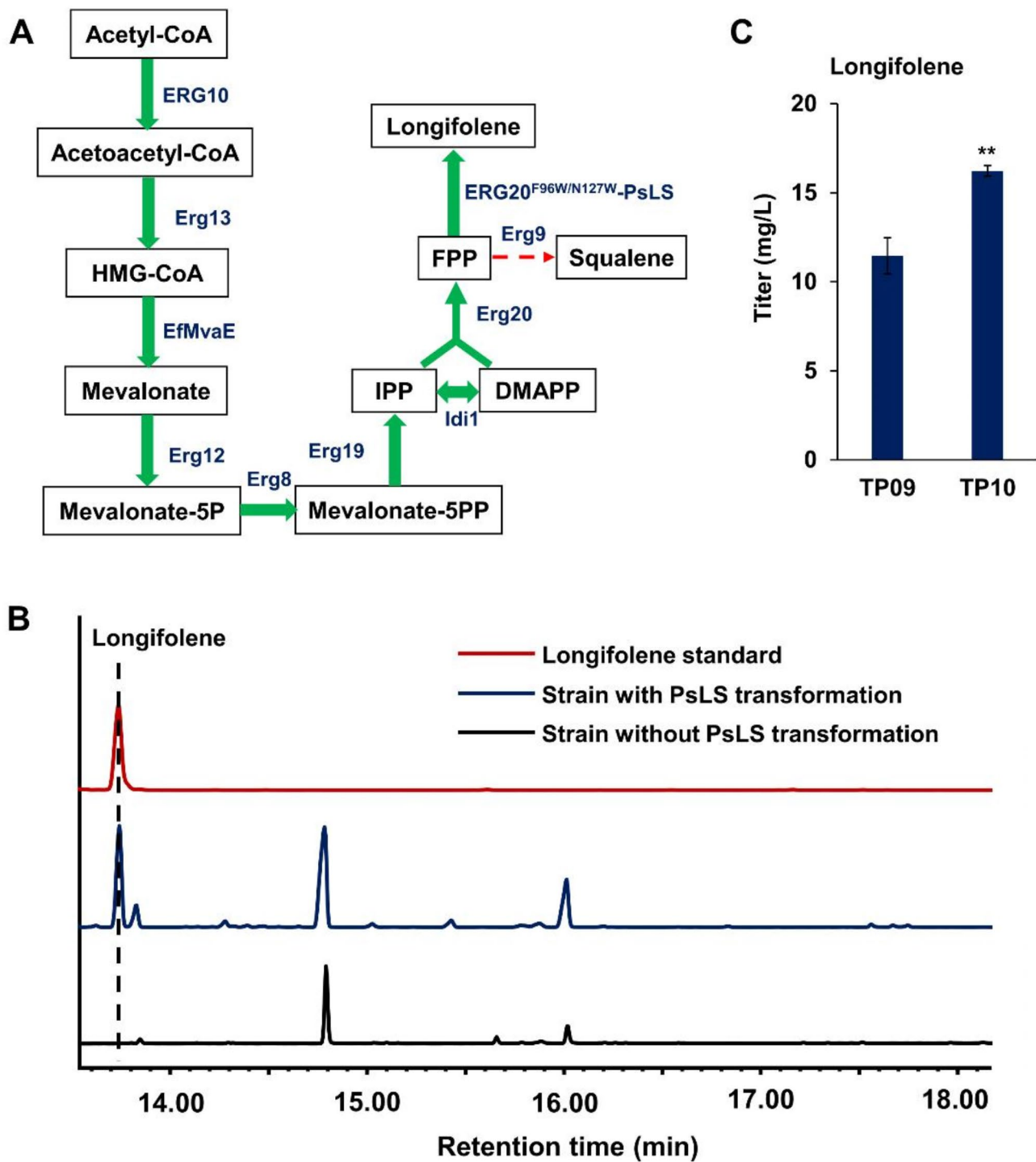


Fig. 6 PCIF1 promoted longifolene production in engineered yeast. **(A)** The optimization of longifolene biosynthesis pathway. Erg10, acetoacetyl-CoA thiolase; Erg13, HMG-CoA synthase; EfMvaE, HMG-CoA reductase from *E. faecalis*; Erg12, mevalonate kinase; Erg8, phosphomevalonate kinase; Erg19, mevalonate pyrophosphate decarboxylase; Idi1, isopentenyl diphosphate: dimethylallyl diphosphate isomerase; Erg20, farnesyl pyrophosphate synthetase; ERG9, squalene synthase; PsLS, codon-optimized longifolene synthase. **(B)** GC-MS detection of longifolene standard and its production in engineered yeast. **(C)** The longifolene production in different yeast strains. The asterisks indicate significant differences (** $p < 0.01$, * $p < 0.05$)

methyltransferase Ime4, in yeast, and the overexpression of this methyltransferase significantly increased the biosynthesis of isoprenoids and aromatic compounds, by significantly elevating the expression of genes in the glycolysis, acetyl-CoA synthesis (PDH bypass) and shikimate/aromatic amino acid synthesis modules [33]. While in this work, the overexpression of PCIF1 increased the production of squalene, and the upregulation of glycolysis was observed, which was different to that in Ime4-overexpressed strain. Thus, the observed effects in PCIF1-overexpressed yeast strain might be specifically due to PCIF1's m⁶Am methyltransferase activity, and we will further verify this in the future.

Conclusion

Here, we reported an efficient engineering method for the biosynthesis of terpenoid in yeast based on m⁶Am modification. The introduction of human m⁶Am methyltransferase PCIF1 into yeast significantly promoted the production of squalene to 2.3-fold increase. Transcriptome analysis revealed that PCIF1 upregulated genes associated with glycolysis and acetyl-CoA biosynthesis pathways. Meanwhile, PCIF1 expression significantly enhanced squalene and sesquiterpenoid longifolene production in engineered yeast strains, with 2.3-fold and 1.4-fold higher increase, respectively. This work provided a PCIF1-based metabolic engineering strategy for the efficient biosynthesis of terpenoids in yeast cell factories.

Supplementary Information

The online version contains supplementary material available at <https://doi.org/10.1186/s12934-025-02701-4>.

Supplementary Material 1

Author contributions

QZ, DL and TA designed the experiment. GW, ML and BF performed the experiments and analyzed the data. XL, JW and YS helped to analyzed the data. GW and TA supervised the work and wrote the manuscript. QZ, DL and TA revised the manuscript. All authors read and approved the final manuscript.

Funding

This work was supported by Shandong Provincial Natural Science Foundation (Grant number ZR2021QC097 and ZR2024QH067) and Introduction and Cultivation Project for Young Creative Talents of Higher Education of Shandong Province.

Data availability

The data supporting this study can be found in this article and supplementary materials. The transcriptome data have been submitted to the NCBI Sequence Read Archive (SRA) database under the accession code PRJNA1155854. All datasets are available from the corresponding author upon reasonable request.

Declarations

Ethics approval and consent to participate

Not applicable.

Consent for publication

Not applicable.

Competing interests

The authors declare no competing interests.

Received: 10 December 2024 / Accepted: 20 March 2025

Published online: 02 April 2025

References

1. Ain QT, Saleem N, Munawar N, Nawaz R, Naseer F, Ahmed S. Quest for malaria management using natural remedies. *Front Pharmacol*. 2024;15:1359890.
2. He W, Liu H, Wu Z, Miao Q, Hu X, Yan X, et al. The AaBBX21-AaHY5 module mediates light-regulated Artemisinin biosynthesis in *Artemisia annua* L. *J Integr Plant Biol*. 2024;66(8):1735–51.
3. Feng Y, An Q, Zhao Z, Wu M, Yang C, Liang W, et al. Beta-elemene: A phytochemical with promise as a drug candidate for tumor therapy and adjuvant tumor therapy. *Biomed Pharmacother*. 2024;172:116266.
4. Zha W, An T, Li T, Zhu J, Gao K, Sun Z, et al. Reconstruction of the biosynthetic pathway of Santalols under control of the GAL regulatory system in yeast. *ACS Synth Biol*. 2020;9(2):449–56.
5. Xia F, Du J, Wang K, Liu L, Ba L, Liu H, et al. Application of multiple strategies to Debottleneck the biosynthesis of longifolene by engineered *Saccharomyces cerevisiae*. *J Agric Food Chem*. 2022;70(36):11336–43.
6. Sukakul T, Uter W, Gonçalo M, Huggard J, Ljubojević Hadžavdić S, Schuttelaar MLA, et al. Results of patch testing with five fragrance materials hitherto not tested: A dose-finding study in the clinical population. *Contact Dermat*. 2024;90(6):566–73.
7. Zhou L, Li J, Zeng T, Xu Z, Luo J, Zheng R, et al. TcMYB8, a R3-MYB transcription factor, positively regulates pyrethrin biosynthesis in *Tanacetum cinerariifolium*. *Int J Mol Sci*. 2022;23(20):12186.
8. Sun R, Xu Y, Liu J, Yang L, Cui G, Zhong G, et al. Proteomic profiling for ovarian development and Azadirachtin exposure in *Spodoptera litura* during metamorphosis from pupae to adults. *Ecotoxicol Environ Saf*. 2022;237:113548.
9. Fan S, Wu M, Liu C, Li H, Huang S, Zheng Z, et al. Azadirachtin inhibits nuclear receptor hr3 in the prothoracic gland to block larval ecdysis in the fall armyworm, *Spodoptera frugiperda*. *J Agric Food Chem*. 2023;71(42):15497–505.
10. Hussain MH, Mohsin MZ, Zaman WQ, Yu J, Zhao X, Wei Y, et al. Multiscale engineering of microbial cell factories: A step forward towards sustainable natural products industry. *Synth Syst Biotechnol*. 2022;7(1):586–601.
11. Li M, Ma M, Wu Z, Liang X, Zheng Q, Li D, et al. Advances in the biosynthesis and metabolic engineering of rare ginsenosides. *Appl Microbiol Biotechnol*. 2023;107(11):3391–404.
12. Lin Y, Wang Y, Zhang G, Chen G, Yang Q, Hao B, et al. Reconstruction of engineered yeast factory for high yield production of ginsenosides Rg3 and Rd. *Front Microbiol*. 2023;14:1191102.
13. Ibrahim GG, Perera M, Abdulmalek SA, Yan J, Yan Y. De novo synthesis of Resveratrol from sucrose by metabolically engineered *Yarrowia lipolytica*. *Biomolecules*. 2024;14(6):712.
14. Gao L, Hou R, Cai P, Yao L, Wu X, Li Y, et al. Engineering yeast peroxisomes for α-bisabolene production from sole methanol with the aid of proteomic analysis. *JACS Au*. 2024;4(7):2474–83.
15. Wu Z, Liang X, Li M, Ma M, Zheng Q, Li D, et al. Advances in the optimization of central carbon metabolism in metabolic engineering. *Microb Cell Fact*. 2023;22(1):76.
16. Wang K, Shi TQ, Wang J, Wei P, Ledesma-Amaro R, Ji X. Engineering the lipid and fatty acid metabolism in *Yarrowia lipolytica* for sustainable production of high oleic oils. *ACS Synth Biol*. 2022;11(4):1542–54.
17. Ye M, Gao J, Li J, Yu W, Bai F, Zhou Y. Promoter engineering enables precise metabolic regulation towards efficient β-elemene production in *Ogataea polymorpha*. *Synth Syst Biotechnol*. 2024;9(2):234–41.
18. Chen M, Song F, Qin Y, Han S, Rao Y, Liang S, et al. Improving thermostability and catalytic activity of glycosyltransferase from *Panax ginseng* by semi-rational design for rebaudioside D synthesis. *Front Bioeng Biotechnol*. 2022;10:884898.
19. Cheah L, Liu L, Stark T, Plan MR, Peng B, Lu Z, et al. Metabolic flux enhancement from the translational fusion of terpene synthases is linked to terpene synthase accumulation. *Metab Eng*. 2023;77:143–51.
20. Cardiff RAL, Carothers JM, Zalatan JG, Sauro HM. Systems-level modeling for CRISPR-based metabolic engineering. *ACS Synth Biol*. 2024;13(9):2643–52.

21. Sveshnikova A, Mohammadi Peyhani H, Hatzimanikatis V. Computational tools and resources for designing new pathways to small molecules. *Curr Opin Biotechnol*. 2022;76:102722.
22. Liyanaarachchi VC, Nishshanka GKSH, Nimarshana PHV, Chang JS, Ariyadasa TU, Nagarajan D. Modeling of Astaxanthin biosynthesis via machine learning, mathematical and metabolic network modeling. *Crit Rev Biotechnol*. 2024;44(6):996–1017.
23. Pandey AK, Park J, Ko J, Joo HH, Raj T, Singh LK, et al. Machine learning in fermentative biohydrogen production: advantages, challenges, and applications. *Bioresour Technol*. 2023;370:128502.
24. Garbo S, D'Andrea D, Colantoni A, Fiorentino F, Mai A, Ramos A, et al. m⁶A modification inhibits MiRNAs' intracellular function, favoring their extracellular export for intercellular communication. *Cell Rep*. 2024;43(6):114369.
25. Jin H, Shi Z, Zhou T, Xie S. Regulation of m⁶Am RNA modification and its implications in human diseases. *J Mol Cell Biol*. 2024;16:mjae012.
26. Xie S, Kuang W, Guo M, Yang F, Jin H, Chen X, et al. m⁶Am methyltransferase PCIF1 negatively regulates ciliation by inhibiting BICD2 expression. *J Cell Biol*. 2024;223(6):e202307002.
27. Schwartz S, Agarwala SD, Mumbach MR, Jovanovic M, Mertins P, Shishkin A, et al. High-resolution mapping reveals a conserved, widespread, dynamic mRNA methylation program in yeast meiosis. *Cell*. 2013;155(6):1409–21.
28. Ensink I, Maman A, Albihlal WS, Lassandro M, Salzano G, Sideri T, et al. The yeast RNA methylation complex consists of conserved yet reconfigured components with m⁶A-dependent and independent roles. *Elife*. 2023;12:RP87860.
29. Li K, Peng J, Yi C. Sequencing methods and functional decoding of mRNA modifications. *Fundam Res*. 2023;3(5):738–48.
30. Schwartz S, Bernstein DA, Mumbach MR, Jovanovic M, Herbst RH, León-Ricardo BX, et al. Transcriptome-wide mapping reveals widespread dynamic-regulated pseudouridylation of ncRNA and mRNA. *Cell*. 2014;159(1):148–62.
31. Varier RA, Sideri T, Capitanchik C, Manova Z, Calvani E, Rossi A, et al. N⁶-methyladenosine (m⁶A) reader Pho92 is recruited co-transcriptionally and couples translation to mRNA decay to promote meiotic fitness in yeast. *Elife*. 2022;11:e84034.
32. Scutenaire J, Plassard D, Matelot M, Villa T, Zumsteg J, Libri D, et al. The *S. cerevisiae* m⁶A-reader Pho92 promotes timely meiotic recombination by controlling key methylated transcripts. *Nucleic Acids Res*. 2023;51(2):517–35.
33. Zhu J, An T, Zha W, Gao K, Li T, Zi J. Manipulation of IME4 expression, a global regulation strategy for metabolic engineering in *Saccharomyces cerevisiae*. *Acta Pharm Sin B*. 2023;13(6):2795–806.
34. Wu Y, Pu X, Wu S, Zhang Y, Fu S, Tang H, et al. PCIF1, the only methyltransferase of N⁶,2'-O-dimethyladenosine. *Cancer Cell Int*. 2023;23(1):226.
35. Sun H, Zhang M, Li K, Bai D, Yi C. Cap-specific, terminal N⁶-methylation by a mammalian m⁶Am methyltransferase. *Cell Res*. 2019;29(1):80–2.
36. Wei C, Gershowitz A, Moss B. N⁶, 2'-O-dimethyladenosine a novel methylated ribonucleoside next to the 5' terminal of animal cell and virus mRNAs. *Nature*. 1975;257(5523):251–53.
37. Cesaro B, Tarullo M, Fatica A. Regulation of gene expression by m⁶Am RNA modification. *Int J Mol Sci*. 2023;24(3):2277.
38. Ben-Haim MS, Pinto Y, Moshitch-Moshkovitz S, Hershkovitz V, Kol N, Diamant-Levi T, et al. Dynamic regulation of N⁶,2'-O-dimethyladenosine (m⁶Am) in obesity. *Nat Commun*. 2021;12(1):7185.
39. Mauer J, Luo X, Blanjoie A, Jiao X, Grozhik AV, Patil DP, et al. Reversible methylation of m⁶Am in the 5' cap controls mRNA stability. *Nature*. 2017;541(7637):371–5.
40. Drazkowska K, Tomecki R, Warminski M, Baran N, Cysewski D, Depaix A, et al. 2'-O-Methylation of the second transcribed nucleotide within the mRNA 5' cap impacts the protein production level in a cell-specific manner and contributes to RNA immune evasion. *Nucleic Acids Res*. 2022;50(16):9051–71.
41. Gao S, Zhou J, Hu Z, Zhang S, Wu Y, Musunuru PP, et al. Effects of the m⁶Am methyltransferase PCIF1 on cell proliferation and survival in gliomas. *Biochim Biophys Acta Mol Basis Dis*. 2022;1868(11):166498.
42. Luo W, Xu Z, Li F, Ding L, Wang R, Lin Y, et al. m⁶Am methyltransferase PCIF1 promotes LPP3 mediated phosphatidic acid metabolism and renal cell carcinoma progression. *Adv Sci (Weinh)*. 2024;11(46):e2404033.
43. Zhao F, Du Y, Bai P, Liu J, Lu W, Yuan Y. Enhancing *Saccharomyces cerevisiae* reactive oxygen species and ethanol stress tolerance for high-level production of Protopanaxadiol. *Bioresour Technol*. 2017;227:308–16.
44. Mishra R, Minc N, Peter M. Cells under pressure: how yeast cells respond to mechanical forces. *Trends Microbiol*. 2022;30(5):495–510.
45. Yuan B, Wang W, Wang Y, Zhao X. Regulatory mechanisms underlying yeast chemical stress response and development of robust strains for bioproduction. *Curr Opin Biotechnol*. 2024;86:103072.
46. Shiba Y, Paradise EM, Kirby J, Ro DK, Keasling JD. Engineering of the pyruvate dehydrogenase bypass in *Saccharomyces cerevisiae* for high-level production of isoprenoids. *Metab Eng*. 2007;9(2):160–68.
47. Krutsakorn B, Imagawa T, Honda K, Okano K, Ohtake H. Construction of an in vitro bypassed pyruvate decarboxylation pathway using thermostable enzyme modules and its application to N-acetylglutamate production. *Microb Cell Fact*. 2013;12:91.
48. Zhang Q, Zeng W, Xu S, Zhou J. Metabolism and strategies for enhanced supply of acetyl-CoA in *Saccharomyces cerevisiae*. *Bioresour Technol*. 2021;342:125978.
49. Lv X, Wang F, Zhou P, Ye L, Xie W, Xu H, et al. Dual regulation of cytoplasmic and mitochondrial acetyl-CoA utilization for improved isoprene production in *Saccharomyces cerevisiae*. *Nat Commun*. 2016;7:12851.
50. Ma M, Li M, Wu Z, Liang X, Zheng Q, Li D, et al. The microbial biosynthesis of noncanonical terpenoids. *Appl Microbiol Biotechnol*. 2024;108(1):226.
51. Yin M, Xu K, Luan T, Kang X, Yang X, Li H, et al. Metabolic engineering for compartmentalized biosynthesis of the valuable compounds in *Saccharomyces cerevisiae*. *Microbiol Res*. 2024;286:127815.
52. Wu J, Cheng S, Cao J, Qiao J, Zhao G. Systematic optimization of limonene production in engineered *Escherichia coli*. *J Agric Food Chem*. 2019;67(25):7087–97.
53. Liu S, Zhang M, Ren Y, Jin G, Tao Y, Lyu L, et al. Engineering *Rhodospiridium toruloides* for limonene production. *Biotechnol Biofuels*. 2021;14(1):243.
54. Zhang Y, Guo J, Gao P, Yan W, Shen J, Luo X, et al. Development of an efficient yeast platform for cannabigerolic acid biosynthesis. *Metab Eng*. 2023;80:232–40.
55. Guo H, Wang H, Chen T, Guo L, Blank LM, Ebert BE, et al. Engineering critical amino acid residues of lanosterol synthase to improve the production of triterpenoids in *Saccharomyces cerevisiae*. *ACS Synth Biol*. 2022;11(8):2685–96.
56. Ignea C, Pontini M, Maffei ME, Makris AM, Kampranis SC. Engineering monoterpene production in yeast using a synthetic dominant negative Geranyl diphosphate synthase. *ACS Synth Biol*. 2014;3:298–06.
57. Hassanien MF, Assiri AM, Alzohairy AM, Oraby HF. Health-promoting value and food applications of black Cumin essential oil: an overview. *J Food Sci Technol*. 2015;52:6136–42.
58. Köpke D, Schröder R, Fischer HM, Gershenzon J, Hilker M, Schmidt A. Does egg deposition by herbivorous Pine? sawflies affect transcription of sesquiterpene synthases in Pine? *Planta*. 2008;228:427–38.
59. Zhuo W, Sun M, Wang K, Zhang L, Li K, Yi D, et al. m⁶Am methyltransferase PCIF1 is essential for aggressiveness of gastric cancer cells by inhibiting TM95F1 mRNA translation. *Cell Discov*. 2022;8(1):48.
60. Wang L, Wu L, Zhu Z, Zhang Q, Li W, Gonzalez GM, et al. Role of PCIF1-mediated 5'-cap N⁶-methyladenosine mRNA methylation in colorectal cancer and anti-PD-1 immunotherapy. *EMBO J*. 2023;42(2):e111673.
61. Zhang Q, Zeng W, Xu S, Zhou J. Metabolism and strategies for enhanced supply of acetyl-CoA in *Saccharomyces cerevisiae*. *Bioresour Technol*. 2021;342:125978.
62. Malci K, Santibáñez R, Jonguitud-Borrego N, Santoyo-García JH, Kerkhoven EJ, Rios-Solis L. Improved production of Taxol® precursors in *S. cerevisiae* using combinatorial in Silico design and metabolic engineering. *Microb Cell Fact*. 2023;22(1):243.
63. Tang M, Xu X, Liu Y, Li J, Du G, Lv X, et al. Combinatorial metabolic engineering for improving betulinic acid biosynthesis in *Saccharomyces cerevisiae*. *ACS Synth Biol*. 2024;13(6):1798–808.
64. Fan J, Zhang Y, Li W, Li Z, Zhang D, Mo Q, et al. Multidimensional optimization of *Saccharomyces cerevisiae* for carotenoid overproduction. *Biodes Res*. 2024;6:0026.
65. Lu Y, Yang Q, Lin Z, Yang X. A modular pathway engineering strategy for the high-level production of β-ionone in *Yarrowia lipolytica*. *Microb Cell Fact*. 2020;19(1):49.
66. Kildegaard KR, Jensen NB, Schneider K, Czarnotta E, Özdemir E, Klein T, et al. Engineering and systems-level analysis of *Saccharomyces cerevisiae* for production of 3-hydroxypropionic acid via malonyl-CoA reductase-dependent pathway. *Microb Cell Fact*. 2016;15:53.

Publisher's note

Springer Nature remains neutral with regard to jurisdictional claims in published maps and institutional affiliations.